Phase Evolution of Solitonlike Optical Pulses during Excitonic Rabi Flopping in a Semiconductor

N. C. Nielsen,* T. Höner zu Siederdissen, and J. Kuhl
Max-Planck-Institut für Festkörperforschung, 70569 Stuttgart, Germany

M. Schaarschmidt, J. Förstner, and A. Knorr
Institut für Theoretische Physik, AG Nichtlineare Optik und Quantenelektronik, Technische Universität Berlin, 10623 Berlin, Germany

H. Giessen
Institute of Applied Physics, University of Bonn, 53115 Bonn, Germany
and 4. Physikalisches Institut, Universität Stuttgart, 70569 Stuttgart, Germany
(Received 6 September 2004; published 9 February 2005)

We demonstrate that the temporal pulse phase remains essentially unaltered before separate phase characteristics are developed when propagating high-intensity pulses coherently on the exciton resonance of an optically thick semiconductor. This behavior is a clear manifestation of self-induced transmission and pulse breakup into solitonlike pulses due to Rabi flopping of the carrier density. Experiments using a novel fast-scan cross-correlation frequency-resolved optical gating (XFROG) method are in good agreement with numerical calculations based on the semiconductor Bloch equations.

DOI: 10.1103/PhysRevLett.94.057406 PACS numbers: 78.47.+p, 42.50.Md, 71.35.Gg, 78.20.Bh

Detailed knowledge of the phase evolution of optical pulses during their interaction with resonant systems is essential for understanding the dynamics of coherent transient phenomena. Rabi flopping of the material polarization is one of the most fundamental examples that is well known from atomic and molecular two-level systems [1–5] and has been rediscovered on exciton transitions in semiconductors [6–8]. In recent years, Rabi flopping has been discussed as a potential scheme for optical quantum processing [9,10], in which the information is carried by the pulse amplitude and phase. So far, most experiments on carrier-density oscillations in semiconductor systems such as multiple quantum wells [11,12] and quantum dots [13,14] were based on indirect measurements of the transient population rather than the propagating pulse itself. However, time-dependent propagation experiments on bulk semiconductors revealed the effects of self-induced transmission and multiple pulse breakup due to Rabi flopping on bound excitons [15] and even on a free-exciton transition [16]. In the latter case, coherent mean-field effects were shown to increase the effective Rabi frequency [17] and to dominate the incoherent effects due to carrier-carrier scattering at high fields and on sufficiently short time scales [18]. The phase information has been disregarded except for a recent experiment on intersubband transitions in doped quantum wells [19]. Here, the reemitted midinfrared field was shown to be alternately in and out of phase with the incident field during the intersubband Rabi oscillations.

In this Letter, we report on the phase evolution of ultrashort pulses during carrier-density Rabi flopping on the free-exciton transition in an optically thick bulk semiconductor. The pulses transmitted in this coherent nonlinear regime exhibit pronounced modulations on the temporal pulse envelope. We will show experimentally and theoretically that the temporal pulse phase remains essentially unaltered before separate phase characteristics are developed, which gives clear evidence of self-induced transmission and pulse breakup into solitonlike pulses. The behavior is opposite to the linear case of polariton propagation [20] as well as to the nonlinear case of self-phase modulation [21], featuring phase jumps of π within the modulated pulse envelope.

The temporal and spectral phases are retrieved by cross-correlation frequency-resolved optical gating (XFROG)

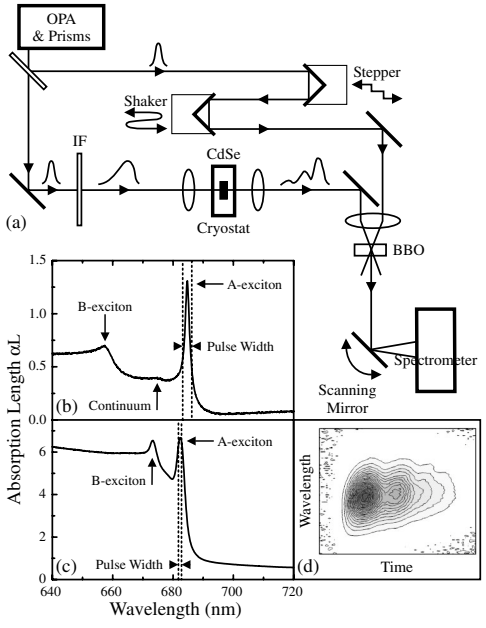

FIG. 1. (a) Fast-scan XFROG setup. (b),(c) Linear absorption spectra of an optically thin and a thick CdSe sample at $T = 8$ K. (d) XFROG trace of a pulse after breakup.

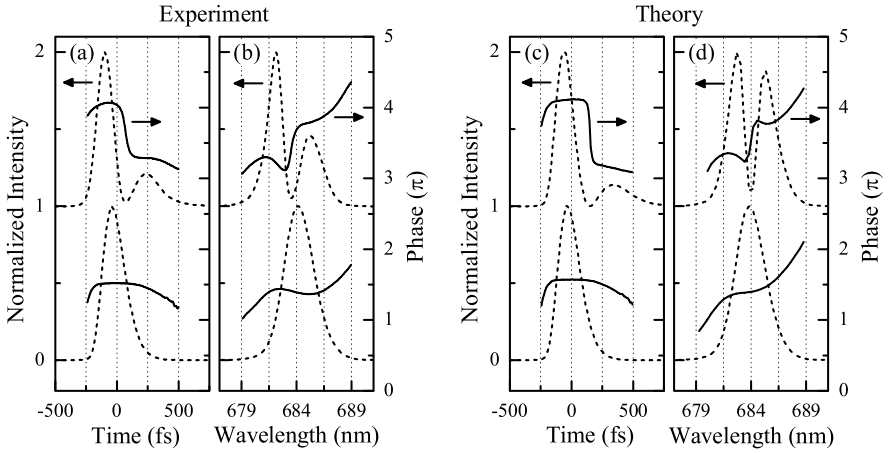

FIG. 2. (a) Experimental temporal and (b) spectral normalized intensity (dashed line) and phase (solid line) for the input pulse (bottom) and after linear propagation through the sample with $\alpha L = 1.3$ at $I = 0.6$ MW/cm^2 (top). (c),(d) Results of the corresponding numerical calculations.

[22], which is a well established method to fully characterize laser pulses. Since standard XFROG setups do not allow multiple signal averaging in short measurement times—which is required in our experiments because of weak signals and a low laser repetition rate—we implemented a new fast-scanning XFROG setup. Until now, similar setups have only been employed for real-time pulse monitoring with second-harmonic generation FROG [23–25]. Figure 1(a) illustrates the experimental setup. We use chirp-free 65 fs pulses, tunable around 683 nm from an optical parametric amplifier (OPA) at a repetition rate of 200 kHz. The cross-correlation scheme involves splitting of the linearly polarized laser output into two portions: One part (33%) passes through a variable delay line, while the second part (67%) is attenuated and focused with an $f = 25$ mm achromat onto the sample which was kept at $T = 8$ K in a cold finger cryostat. Insertion of a bandpass filter before the sample narrowed the broad spectrum to the width of the exciton resonance, thereby lengthening the pulse. Subsequently, both parts are overlapped in a 1-mm-thick β-barium-borate (BBO) crystal. The XFROG trace is recorded by an imaging spectrometer with a charge coupled device (CCD) camera. A galvanometric scanning mirror in front of the spectrometer entrance slit is synchronized with the periodic movement of the shaker in the delay line. Thus, the vertical axis of the CCD array can be used as the time axis together with the horizontal wavelength axis. The discrete translations of a stepper in the delay line are used for the time-base calibration. At an operation frequency of 60 Hz, we achieved high signal-to-noise ratio and low retrieval errors of the XFROG algorithm.

The experiments were performed on two CdSe bulk crystals grown by hot-wall epitaxy on transparent BaF_2 substrates. We used an optically thin CdSe sample with absorption length $\alpha L = 1.3$ to study propagation effects in the linear excitation regime, and an optically thick CdSe sample with $\alpha L = 6.7$ to investigate the characteristics of coherent nonlinear transmission. The c axis of the CdSe was oriented perpendicularly to the substrate. Thus, both the intrinsic A- and B-exciton resonances could be excited with linearly polarized light normally incident to the sample ($\mathbf{E} \perp \mathbf{c}$). Figs. 1(b) and 1(c) show the corresponding absorption spectra at $T = 8$ K.

For the theoretical description of the linear and nonlinear light propagation effects, Maxwell's equations have been evaluated using the slowly varying envelope approximation [5,26]. The dipole density, which is a source term in Maxwell's equations, is calculated using the semiconductor Bloch equations in the Hartree-Fock limit [27]. We employed an effective phenomenological damping $\hbar\gamma = 2$ meV to account for all present scattering mechanisms which have been calculated in Ref. [16]. We explain the suitability of the phenomenologically damped Hartree-Fock theory also with the fact that the Coulomb collision efficiency is drastically decreased by light dressing [28], which leads to a smaller deviation. Our approach allows to reproduce the observed excitonic self-induced transmission and multiple pulse breakup. The combined semiconductor Maxwell-Bloch equations can be numerically evaluated for arbitrary shapes, strength, and duration of the input pulse. For the presented calculations, the input pulse from the experiment was modeled to appropriately take into account the asymmetry and chirp properties of the real pulse. The strength of the pulse, i.e., the ability to induce nonlinear effects, is given by the pulse area $\theta = \int_{-\infty}^{\infty}(d_{cv}/\hbar)|E(t)|dt$ at the beginning of the sample. Here, d_{cv} is the interband transition dipole element and $|E(t)|$ is the amplitude of the field. The numerical parameters for the calculations have been derived from the linear propagation experiment.

The intensity and phase characteristics in the linear regime of polariton propagation are illustrated in Fig. 2. We measured XFROG traces for the propagation of 210 fs pulses resonantly tuned to the A-exciton transition of the thin CdSe sample with $\alpha L = 1.3$ at $T = 8$ K. The XFROG traces were recorded with an integration time of 5 min and retrieved from a 256×256 grid yielding FROG errors of less than 0.003. The retrieved normalized intensity and phase in the temporal and spectral domain are shown in Figs. 2(a) and 2(b), respectively. The lower curves characterize the input pulse as measured after propagation

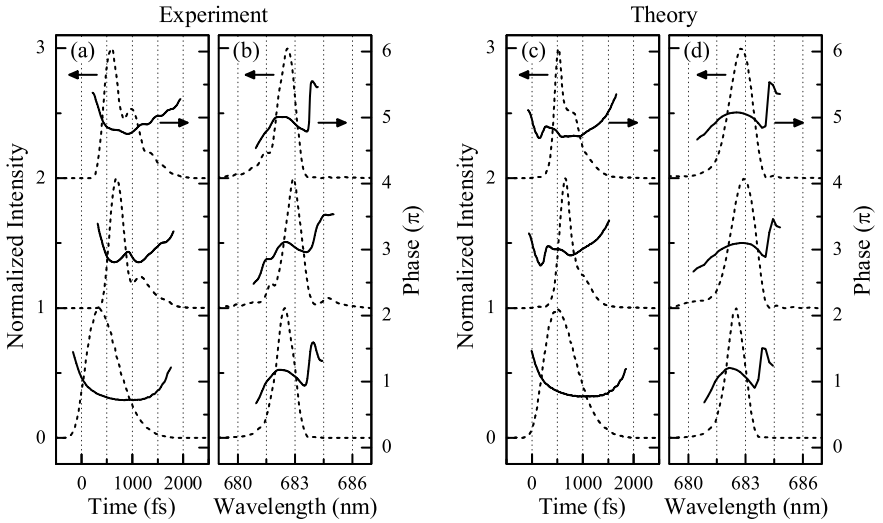

FIG. 3. (a) Experimental temporal and (b) spectral normalized intensity (dashed line) and phase (solid line) for the input pulse (bottom) and after nonlinear propagation through the sample with $\alpha L = 6.7$ at $I = 780\ \mathrm{MW/cm^2}$ (middle) and $1.2\ \mathrm{GW/cm^2}$ (top). (c), (d) Results of the corresponding numerical calculations for a pulse area $\theta = 2.0\pi$ (middle) and 2.6π (top).

through the sample substrate, featuring a roughly single-sided exponential envelope and (according to the sign conventions) a slight positive chirp caused by the employed Lorentzian bandpass filter (IF) with 3 nm bandwidth and additional blocking section. This bandwidth ensures the excitation of both polariton branches, i.e., of a spectral range around the A-exciton resonance [compare Fig. 1(b)]. The pulses propagate linearly through the sample at an intensity of $I = 0.6\ \mathrm{MW/cm^2}$ (upper curves) and exhibit a distinct splitting into two pulse components separated by approximately 340 fs in time. The corresponding spectrum reveals two spectral components on both sides of the A-exciton resonance that are transmitted through the sample and transform into the temporal beating between two polariton branches [29]. As expected for a beating phenomenon, the temporal phase shows a phase jump of almost π between both pulse components, which is equivalent to a change of sign of the field. Before and after the phase jump, the curve follows the input pulse phase. The spectral phase distortion is a measure of the refractive index dispersion around resonance [30], which could be used to accurately describe the material system. The polariton beating as well as the spectral phase are well reproduced by the theoretical calculations [Figs. 2(c) and 2(d)].

The phase evolution in the nonlinear regime of self-induced transmission is studied using 730 fs pulses that are resonant to the A-exciton of the optically thick CdSe sample with $\alpha L = 6.7$, i.e., a linear transmission of about 0.001. Thus, propagation of low-intensity light is largely inhibited, and coherent pulse breakup can clearly evolve over the propagation distance. The lower curves in Figs. 3(a) and 3(b) illustrate the roughly single-sided exponential input pulse, which was tailored using a Lorentzian bandpass filter with 1 nm bandwidth. Here, a slightly negative chirp applies. The small bandwidth is required to excite only a narrow distribution within the (inhomogeneously) broadened A-exciton resonance [compare Fig. 1(c)]. For the propagation at $I = 780\ \mathrm{MW/cm^2}$ (middle curves), temporal reshaping, steepening, and breakup into two distinct pulse components occur. At $I = 1.2\ \mathrm{GW/cm^2}$ (upper curves), further steepening and a third pulse component can be identified. In both cases, we do not find remarkable distortions in the spectral domain except for a modest asymmetric broadening on the high-energy side. These temporal and spectral properties in addition to the nonlinear transmission of up to 25% (corrected for surface reflectivity) indicate Rabi flopping as expected for a growing pulse area. In contrast to the linear experiments, the nonlinear pulse breakup is accompanied by a temporal phase that essentially follows the quadratic input phase [Fig. 3(a)]. Slight phase modulations of less than 0.2π occur synchronously with the temporal pulse breakup. In the spectral domain, the phase of the transmitted pulses roughly corresponds to the input pulse phase [Fig. 3(b)]. For the $1.2\ \mathrm{GW/cm^2}$ pulse, a phase jump of $-\pi$ on the low-energy side of the spectral peak was obtained in seven out of ten retrievals instead of the displayed phase jump of $+\pi$. Both results of the retrieval are, however, almost equivalent.

Figs. 3(c) and 3(d) show the results of the corresponding numerical simulations. The input pulse (lower curves) was modeled according to the experimental conditions. The transmitted pulses (middle and upper curves) were calculated for an input pulse area θ increasing by a factor of 1.3 from 2.0π to 2.6π. Note for comparison that the intensity goes as pulse area squared and that the area values agree with the measured intensities if a dipole moment of about 1.5 eÅ is assumed. The experimental findings are well reproduced. The excitation-dependent temporal pulse breakup due to Rabi flopping of the carrier density can be observed as well as a phase characteristic that essentially follows the input phase profile except for slight modulations [Fig. 3(c)]. These phase modulations are explained with the coherent reemission of light during the Rabi flopping. The emission is accelerated or decelerated depending on the field gradient, and the temporal phase is correspondingly compressed or stretched. Thus, pulse breakup and formation of individual solitonlike pulses

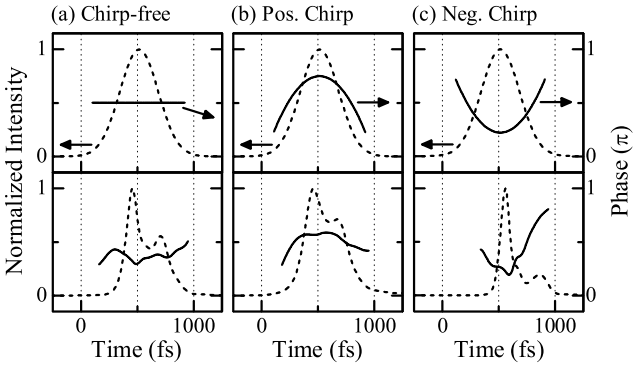

FIG. 4. (a)–(c) Theoretical plots of temporal intensity (dashed line) and phase (solid line) for the 400 fs Gaussian input pulse (top) and after nonlinear propagation according to the experiment with a pulse area $\theta = 2.6\pi$ (bottom). (a) Chirp-free, (b) positive chirp, and (c) negative chirp.

manifest themselves clearly in the development of separate phase characteristics for each pulse component. The asymmetric spectra shown in Fig. 3(d) marginally change with increasing pulse area. The respective spectral phases are nearly invariant.

To investigate the influence of the input pulse chirp and to clarify the nature of the slight phase modulations, we performed numerical calculations for different pulse chirp and propagation lengths. The normalized intensity and phase characteristics of the 400 fs Gaussian input and transmitted pulses after nonlinear propagation according to the experiment with a pulse area of 2.6π are depicted in Fig. 4. For chirp-free input pulses [Fig. 4(a)], we find temporal pulse breakup and a flat output phase with slight modulations as described in the preceding paragraph. For chirped input pulses [Figs. 4(b) and 4(c)], the transmitted pulse shape is altered due to the different relative velocity of the pulse components after breakup. Here, the output phase is given mainly by the quadratic input phase superimposed by the modulations already apparent in the chirp-free case. For a significantly longer propagation distance, pulse breakup into well-separated solitonlike pulses occurs. The input chirp determines the relative delay of the individual pulses. Each pulse is characterized by a temporal phase that features a flat section at the position of the pulse peak surrounded by the phase deviations in the course of Rabi flopping. The development of separate phase characteristics without a defined phase relation is in contrast to the linear polariton beating with phase jumps of π between the discrete pulse components [compare Figs. 2(a) and 2(c)].

In conclusion, we have presented the phase evolution of ultrashort pulses during carrier-density Rabi flopping on the exciton transition of an optically thick semiconductor. The pulses transmitted in this coherent nonlinear regime exhibit pronounced modulations on the temporal envelope. Here, we have shown in a novel XFROG experiment and by theoretical modeling based on semiconductor Maxwell-Bloch theory that the temporal phase remains essentially unaltered before separate phase characteristics are developed, which gives clear evidence of self-induced transmission and pulse breakup into solitonlike pulses. The behavior is opposite to the linear case of polariton propagation and the nonlinear case of self-phase modulation, featuring phase jumps of π within the modulated pulse envelope.

The authors would like to thank M. Grün and M. Hetterich for providing the high-quality CdSe samples. The Berlin group would like to thank the DFG for financial support through the SFB 296. H. G. would like to thank the DFG (SPP 1113 and FOR 557) and BMBF (13N8340) for support.

*Electronic address: n.nielsen@fkf.mpg.de

[1] S. L. McCall and E. L. Hahn, Phys. Rev. Lett. **18**, 908 (1967).
[2] L. Matulic, Opt. Commun. **2**, 249 (1970).
[3] H. M. Gibbs and R. E. Slusher, Phys. Rev. Lett. **24**, 638 (1970).
[4] G. L. Lamb, Jr., Phys. Rev. Lett. **31**, 196 (1973).
[5] L. Allen and J. H. Eberly, *Optical Resonance and Two-Level Atoms* (Dover, New York, 1987).
[6] R. Binder *et al.*, Phys. Rev. Lett. **65**, 899 (1990).
[7] S. W. Koch *et al.*, Phys. Status Solidi B **173**, 177 (1992).
[8] H. Haug and S. W. Koch, *Quantum Theory of the Optical and Electronic Properties of Semiconductors* (World Scientific, Singapore, 1994).
[9] M. A. Nielsen and I. L. Chuang, *Quantum Computation and Quantum Information* (Cambridge University Press, Cambridge, England, 2000).
[10] X. Li *et al.*, Science **301**, 809 (2003).
[11] S. T. Cundiff *et al.*, Phys. Rev. Lett. **73**, 1178 (1994).
[12] A. Schülzgen *et al.*, Phys. Rev. Lett. **82**, 2346 (1999).
[13] T. H. Stievater *et al.*, Phys. Rev. Lett. **87**, 133603 (2001).
[14] A. Zrenner *et al.*, Nature (London) **418**, 612 (2002).
[15] M. Jütte, H. Stolz, and W. von der Osten, J. Opt. Soc. Am. B **13**, 1205 (1996).
[16] H. Giessen *et al.*, Phys. Rev. Lett. **81**, 4260 (1998).
[17] Th. Östreich and A. Knorr, Phys. Rev. B **48**, 17811 (1993).
[18] N. C. Nielsen *et al.*, Phys. Rev. B **64**, 245202 (2001).
[19] C. W. Luo *et al.*, Phys. Rev. Lett. **92**, 047402 (2004).
[20] J. S. Nägerl *et al.*, Phys. Rev. B **63**, 235202 (2001).
[21] F. G. Omenetto *et al.*, Opt. Lett. **24**, 1392 (1999).
[22] S. Linden, H. Giessen, and J. Kuhl, Phys. Status Solidi B **206**, 119 (1998).
[23] D. T. Reid *et al.*, Appl. Opt. **36**, 9103 (1997).
[24] D. O'Shea *et al.*, Opt. Lett. **26**, 1442 (2001).
[25] J. Garduño-Mejía *et al.*, Rev. Sci. Instrum. **74**, 3624 (2003).
[26] A. Knorr *et al.*, Phys. Rev. A **46**, 7179 (1992).
[27] M. Lindberg and S. W. Koch, Phys. Rev. B **38**, 3342 (1988).
[28] C. Ciuti *et al.*, Phys. Rev. Lett. **84**, 1752 (2000).
[29] D. Fröhlich *et al.*, Phys. Rev. Lett. **67**, 2343 (1991).
[30] Y. Mitsumori *et al.*, J. Lumin. **94**, 645 (2001).